Validation of an Actuator Line Model Coupled to a Dynamic Stall Model for Pitching Motions Characteristic to Vertical Axis Turbines

Victor Mendoza[1], Peter Bachant[2], Martin Wosnik[2] and Anders Goude[1]

[1] Department of Engineering Sciences, Division of Electricity, Uppsala University, Uppsala 751 21, Sweden
[2] Center for Ocean Renewable Energy, University of New Hampshire, 24 Colovos Rd., Durham, NH 03824, USA

E-mail: victor.mendoza@angstrom.uu.se

Abstract. Vertical axis wind turbines (VAWT) can be used to extract renewable energy from wind flows. A simpler design, low cost of maintenance, and the ability to accept flow from all directions perpendicular to the rotor axis are some of the most important advantages over conventional horizontal axis wind turbines (HAWT). However, VAWT encounter complex and unsteady fluid dynamics, which present significant modeling challenges. One of the most relevant phenomena is dynamic stall, which is caused by the unsteady variation of angle of attack throughout the blade rotation, and is the focus of the present study. Dynamic stall is usually used as a passive control for VAWT operating conditions, hence the importance of predicting its effects. In this study, a coupled model is implemented with the open-source CFD toolbox OpenFOAM for solving the Navier–Stokes equations, where an actuator line model and dynamic stall model are used to compute the blade loading and body force. Force coefficients obtained from the model are validated with experimental data of pitching airfoil in similar operating conditions as an H-rotor type VAWT. Numerical results show reasonable agreement with experimental data for pitching motion.

1. Introduction

Operating conditions of Vertical Axis Wind Turbines (VAWT) are characterized as complex unsteady flows which give a considerable challenge, both to describe using measurements and to represent through simulation tools [1]. Moreover, VAWT blades are inherently exposed to cyclic variation in the angle of attack, which gives cyclic blade forces and can give material fatigue damage. Accurate modeling of the varying forces is therefore very important for the design of the VAWT.

The amplitude of the angle of attack oscillation in a fixed pitch VAWT is increasing with decreased tip speed ration (TSR), and at low TSR (common during stall regulation), the blades will experience dynamic stall, where the force coefficients for the blade not only depend on the angle of attack, but also on the rate of change of the angle of attack. The aim of this study is to investigate the performance of a Leishman-Beddoes type dynamic stall model when implemented within an actuator line model, for pitching motion typical to a VAWT.

2. Methodology

For solving the governing equations of the phenomena involved, a coupled model has been implemented: the actuator line model (ALM) samples the flow velocity from the Navier–Stokes solver, and thereby computes each blade element's angle of attack and relative velocity. The dynamic stall model is used to calculate blade force coefficients, which the actuator line model uses to impart the body force back into the flow solver.

In this work, it was chosen to validate the model against wind tunnel data for a pitching blade. This will put the focus on the force modeling part in the simulation model.

2.1. Actuator Line Model

The ALM is a three-dimensional and unsteady aerodynamic model developed by Sørensen and Shen [2], used to study the flow around wind turbines. It is a combination of a solver of the Navier–Stokes equations with a so-called actuator line technique, in which blades of the turbine are represented by a distribution of body forces along lines. These forces are determined using a dynamic stall model commonly based on empirical data. This work uses the library turbinesFoam developed by Bachant et al. [3–5].

The model employed here is based on the incompressible Navier–Stokes equation

$$\frac{\partial \vec{V}}{\partial t} + \vec{V} \cdot \nabla \vec{V} = -\frac{1}{\rho}\nabla p + \nu \nabla^2 \vec{V} + \vec{f} \tag{1}$$

with $\vec{f}$ representing the body forces, which are the loads on the rotating blades for this case.

Static lift and drag coefficients of the 2D profile used for this study are taken from the technical report by Sheldahl and Klimas [6], which is a popular database containing values for a wide range of Reynolds numbers. These coefficients are tabulated and combined with the blade element approach for determining body forces acting on blades. Relative flow velocity $\vec{V}_{\text{rel}}$ and angle of attack α are calculated for each blade using the geometric relation between the velocity of the blade $-\Omega r$, with Ω representing the angular (rotational) velocity of the rotor and r the radius of the blade element, and the velocity of the local incident wind flow $\vec{V}_{\text{in}}$ which is generally lower than the incoming flow velocity $\vec{V}_{\infty}$. Figure 1 depicts a cross-sectional airfoil element at radius r in the plane perpendicular to the turbine axis.

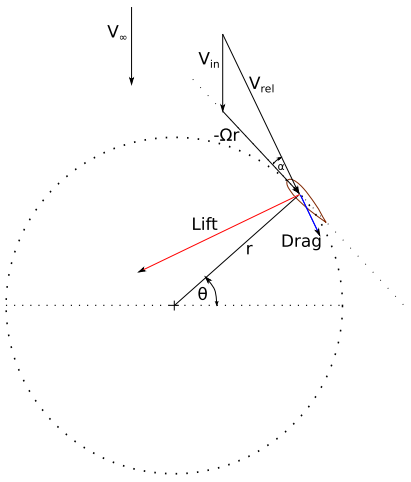

Figure 1. Illustration of velocity vectors and forces acting at the cross-section airfoil element

Once the angle of attack, relative velocity are obtained, the blade element lift and drag forces per spanwise length unit are calculated as

$$f_L = \frac{1}{2}\,\rho\,c\,C_L\,|V_{\text{rel}}|^2 \tag{2}$$

$$f_D = \frac{1}{2}\,\rho\,c\,C_D\,|V_{\text{rel}}|^2 \tag{3}$$

where C_L and C_D are the lift and drag coefficients, respectively. Both are function of the Reynolds number and the angle of attack. It should be emphasized that the direction of the lift and drag are respectively perpendicular and parallel to the relative velocity $\vec{V}_{\text{rel}}$. c represents the chord length.

Same procedure is used to calculate forces from the turbine shaft and blade support struts. After all these forces on the actuator lines are calculated, then are added as a body force source, per unit of density (incompressible assumption), in the momentum Navier–Stokes equations (equation 1).

Calculated force distribution

The applied forces in the ALM need to be distributed smoothly on several mesh points in order to avoid instability due to high gradients. Source term forces should be projected around the element location using a three-dimensional Gaussian kernel. This gives the smoothing function η, which is multiplied by the computed local force on the actuator line element and then imparted on a cell with a distance $|\vec{r}|$ from the actuator line element quarter chord location:

$$\eta = \frac{1}{\epsilon^3\pi^{3/2}}\exp\left[-\left(\frac{|\vec{r}|}{\epsilon}\right)^2\right]$$

The smoothing width parameter ϵ is chosen by the maximum value from three contributions: one relative to the 25% of the chord length, one to the mesh size, and one to the momentum thickness due to drag force, and it is expressed as:

$$\epsilon = \max\left[\frac{c}{4}, 4\sqrt[3]{V_{\text{cell}}}, \frac{cC_D}{2}\right]$$

Where V_{cell} is the cell volume. More details about force projection are in [4].

2.2. Dynamic Stall Modeling

The dynamic stall model (DSM) is represented by the Leishman-Beddoes model [7] with the modifications of Sheng et al. [8] and Dyachuk [9]. It is capable to calculate the unsteady lift, pitching moment and drag, giving a physical description of the aerodynamics. It have been validated with experimental data in [10]. The model is separated into three subsystems: an attached flow model for unsteady linear airloads, a separated flow model for non-linear airloads and a dynamic stall model for the airloads induced by the leading edge vortex.

The unsteady attached flow solution considers the circulatory and impulsive loads, which, at the same time depend on the unsteady bound vortex. The circulatory normal force coefficient could be expressed as

$$C^C_{N_n} = C_{N_\alpha}\alpha_{E_n} \tag{4}$$

where $C_{N\alpha}$ indicates the slope of the static normal force coefficient for a specific Reynolds number, and α_{E_n} is an expression for an equivalent angle of attack

$$\alpha_{E_n} = \alpha_n - X_n - Y_n - Z_n \tag{5}$$

where α is the geometrical angle of attack and X, Y and Z are the deficiency functions, which are empirically derived, based on the flow velocity and the pitching rate, the details are found in [11]. Indices n and $n-1$ represent the current and previous time-step. A delayed angle of attack is considered due to the lag in pressure response, and it is calculated as

$$\alpha_n{}' = \alpha_n - D_{\alpha_n} \tag{6}$$

with D_α as the deficiency function

$$D_{\alpha_n} = D_{\alpha_{n-1}} \exp\left(-\frac{\Delta s}{T_\alpha}\right) + (\alpha_n - \alpha_{n-1}) \exp\left(-\frac{\Delta s}{2T_\alpha}\right) \tag{7}$$

with the empirically derived time constant T_α, which has a value of $T_\alpha = 6.3$ for the NACA0021 airfoil, and Δs corresponds to a non-dimensional time-step

$$\Delta s = \frac{2|\vec{V}_{rel}|\Delta t}{c}. \tag{8}$$

Because of the reversal flow in the boundary layer, a leading edge vortex is created at the surface of the airfoil. The critical angle of attack α_{cr_n} defines the condition at which dynamic stall begins

$$\alpha_{cr_n} = \begin{cases} \alpha_{ds0} & |r_n| \geqslant r_0 \\ \alpha_{ss} + (\alpha_{ds0} - \alpha_{ss})\frac{|r_n|}{r_0} & |r_n| < r_0 \end{cases} \tag{9}$$

with the reduced pitching rate r_n defined as

$$r_n = \frac{\dot{\alpha}_n c}{2|\vec{V}_{rel}|} \tag{10}$$

here, $\dot{\alpha}$ is the pitch rate, r_0 is the reduced pitching rate, which limits the quasi-steady stall with the dynamic stall. Its value is $r_0 = 0.01$ for the NACA0021 airfoil. The static stall onset angle α_{ss} and the critical stall onset angle α_{ds0} are 14.33 and 17.91, respectively. The following is the the dynamic stall condition used

$$|\alpha'| > \alpha_{cr} \rightarrow \text{stall} \tag{11}$$

for the separated flow, the effects are divided in two groups: trailing edge separation and leading vortex convection. The first one is related to the time delay in the movement of the boundary separation point, and is calculated using Kirchhoff's approximation

$$f'_n = \begin{cases} 1 - 0.4\exp\left(\frac{|\alpha'_n| - \alpha_1}{S_1}\right) & |\alpha'_n| < \alpha_1 \\ 0.02 - 0.58\exp\left(\frac{\alpha_1 - |\alpha'_n|}{S_2}\right) & |\alpha'_n| \geqslant \alpha_1 \end{cases} \tag{12}$$

where f' is the delayed separation point and α_1, S_1 and S_2 are constant based on the airfoil profile and the local Reynolds number, these can be found in [11]. The boundary layer around

the blade is in function on the time, and this effect is superimposed on the pressure response delay. The additional delay is represented by f'', which is the dynamic separation point

$$f''_n = f'_n - D_{f_n} \tag{13}$$

and D_{f_n} is the deficiency function defined as

$$D_{f_n} = D_{f_{n-1}} \exp\left(-\frac{\Delta s}{T_f}\right) + (f_n - f_{n-1}) \exp\left(-\frac{\Delta s}{2T_f}\right) \tag{14}$$

Here, T_f is empirically derived time constant and its value is $T_f = 3$. Then, the normal force coefficient for unsteady conditions before the dynamic stall onset is calculated as

$$C^f_{N_n} = C_{N_\alpha} \alpha_{E_n} \left(\frac{1 + \sqrt{f''_n}}{2}\right)^2 \tag{15}$$

after the stall condition is met, the leading edge vortex convects over the surface of the airfoil towards the trailing edge. A significant increase in the normal forces occurs during this process

$$C^v_N = B_1(f''_n - f_n)V_x \tag{16}$$

where C^v_N represents the normal force coefficient during the vortex convection, which is in function of the pitch rate. V_x and B_1 are parameters based on the local Reynolds number and the airfoil profile, they are found in [11]. Once the vortex passes the trailing edge, the normal force decreases quickly. Total normal force obtained is expressed as

$$C_N = C^f_{N_n} + C^v_N \tag{17}$$

Figure 2 shows an example of the normal coefficient forces on a blade during pitching motion, using the above model described.

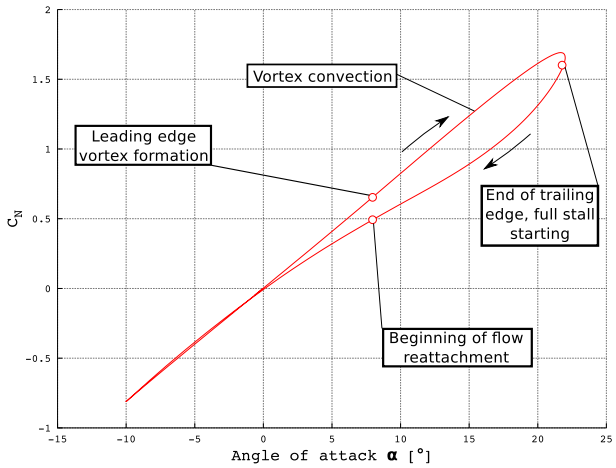

Figure 2. Illustration of dynamic stall: NACA0021 profile with $\alpha = 6 + 16\sin(\Omega t)$, $\Omega = 12,47$[rad/s], $V_\infty = 34,3$[m/s] and $c = 0{,}55$[m]

Tangential force coefficient is calculated trough Kichhoff's flow relation using the dynamic separation point.

$$C_T = \eta C_{N_\alpha} \alpha^2_E (\sqrt{f''_n} - E_0) \tag{18}$$

with the empirical constants $\eta = 0.975$ and $E_0 = 0.15$ corresponding to NACA0021 airfoil profile.

3. Simulation Parameters: Validation case

A NACA0021 airfoil was tested at the Reynolds number of 1.000.000 (which is a reasonable value for operating VAWT) during pitching motion similar to the motion of the VAWT blade. Different pitching amplitudes were investigated: 13.8, 17.4 and 22.6°, analog to a TSR of $\lambda =$ 4.19, 3.34 and 2.6 respectively (see equation 20), to cover a wide range of operational conditions of a VAWT. In a VAWT with fixed blades, the angle of attack is in function of the TSR of the turbine. A periodic function is used to represent the variations of the angles of attack which a VAWT blade experiences analog to the pitching motion,

$$\alpha = \arctan\left(\frac{\sin\theta}{\lambda + \cos\theta}\right) \tag{19}$$

where θ is the azimuthal blade angle and λ represents the TSR,

$$\lambda = \frac{\Omega R}{|\vec{V}_\infty|} \tag{20}$$

In the equation 19, α represents the geometric angle of attack, and it is different to the effective angle of attack α_E, which is calculated by the model in order to get the force coefficients. A NACA0021 profile with 0.55[m] of chord length is driven to the dynamic stall region trough the pitching motion accordint to equation 19. The pitching blade experiments were carried out at Glasgow University [12].

4. Results and discussion

In this section, obtained results for C_N and C_T from simulations are compared with the experimental data. Varying parameters have been tested, mainly in the deep stall condition for an amplitude of 22.6 ° (equivalent to $\lambda = 2.6$). All the studied cases were simulated with a domain geometrically similar to the wind tunnel used in [12] to emulate the pitching blade experiments: 1.61[m] of span, 2.13[m] of height, 2.5[m] upstream and 4[m] downstream, with similar velocity boundary conditions: 28.4[m/s] in the inlet and no-slip condition (fixed 0[m/s]) in the walls, using a LES Smagorinsky turbulence model. Figure 3 shows that the model needs two revolutions to reach the convergence, a third revolution will not produce any change.

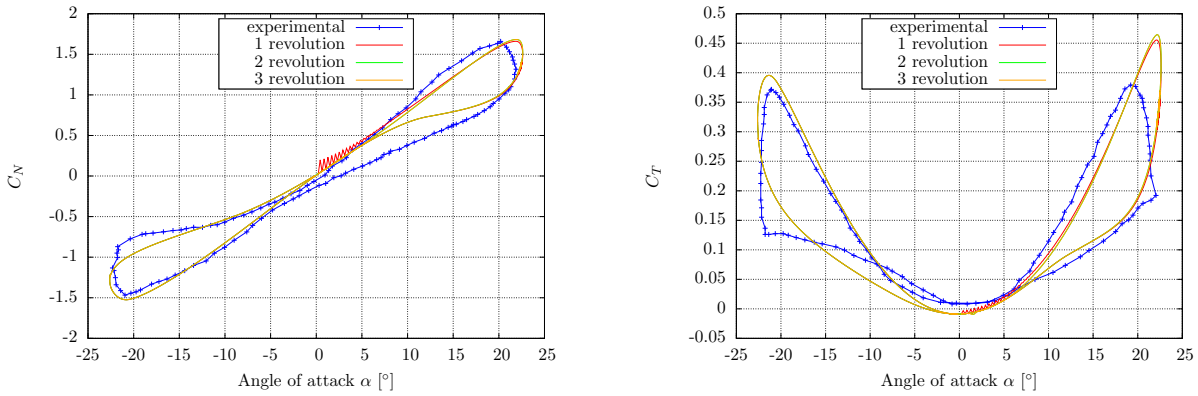

Figure 3. Normal (left) and tangential (right) force coefficients varying the number of revolutions for a pitching motion of NACA0021 airfoil with a maximum amplitude of 22.6°.

Spatial sensitivity: A test of the response of the model to the variation in the size of the mesh is carried out. A mesh of approximatively 1e5 of cells with a local refinement around

the blade is used as a reference mesh (Figure 4), this topology is kept constant and globally refinement are applied for this study; it means the mesh is proportionally scaled in every coordinates.

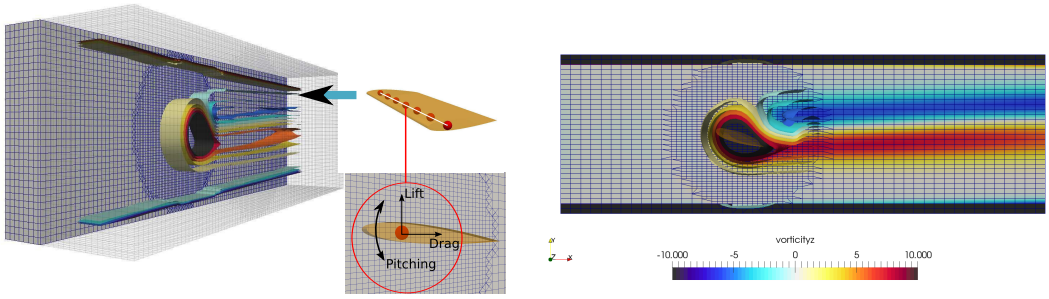

Figure 4. Illustration of a reference mesh section and vorticity isosurfaces generated by the pitching motion around the blade.

From Figure 5, it could be noticed that there is a variation in the results either for a decreasing or increasing in the mesh resolution. Between the refinement of 150 and 200% not considerable changes are obtained in the results, so a major refinement is not justified due this will not give any possible improvement in the accuracy of the results.

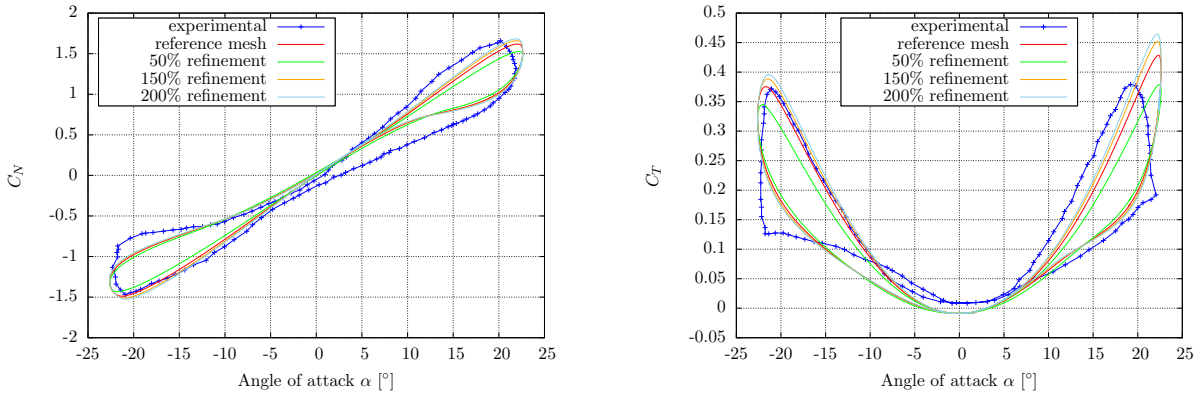

Figure 5. Normal (left) and tangential (right) force coefficients varying the size of the reference mesh for a pitching motion with a maximum amplitude of 22.6°

Temporal sensitivity: Different time-steps were chosen for a varying temporal discretization test, which Δt values are 0.001, 0.003, 0.0055 and 0.0075[s], and these correspond to around 1200, 400, 220 and 160 time-steps per revolution respectively. In this study a coarse mesh with a refinement of 25%, compared to the reference one, was used. Results are shown in Figure 6.

The model is more sensitive to the spatial discretization than the temporal one; same characteristic was obtained by Bachant et al. in [4]. Accuracy and stability were not affected even for big values for Δt, as long they are within the limit given by the CFL condition; a Courant number of less than unity is required. On the other hand, it should be considered that small time-step of discretization could cause numerical instabilities due to the fluctuation of the flow fields resolving the transient term $\frac{\partial \alpha}{\partial t}$.

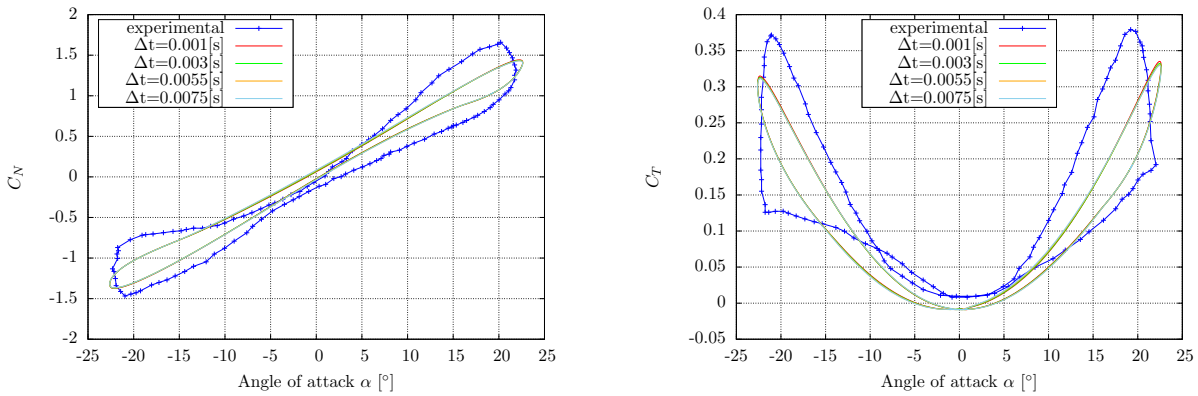

Figure 6. Normal (left) and tangential (right) force coefficients varying time-step discretization for a pitching motion with a maximum amplitude of 22.6°

4.1. TSR Variation

For a TSR of 4.19 (Figure 7), peaks values for both C_N and C_T are similar to experiments. In this condition, the flow is attached and the blades are not in the stall region. Therefore, model have good agreement with experimental data using unsteady attached angle of attack calculation.

For a TSR of 3.34 (Figure 8), the maximum magnitude of the angle of attack is at 17.4° which is in the stall region. Both C_N and C_T curves show the delay of the flow reattachment, which is characteristic of the dynamic stall phenomenon. Peaks of simulated values have close agreement with the measured data. The stall onset angle flow reattachment are well predicted.

For a TSR of 2.60 (Figure 9), the maximum amplitude of the angle of attack is 22.6°, which is related to a deeper stall region compared to a TSR of 3.34. This is shown because the "loop" of the curve is wider for the lower TSR, and moreover, the reattachment of the flow is further delayed. Simulated peak for C_T is overestimated.

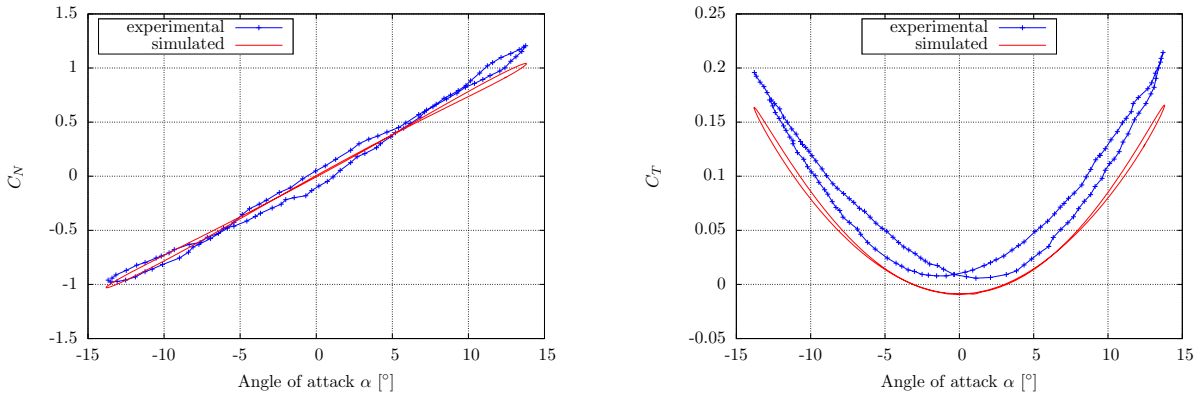

Figure 7. Normal (left) and tangential (right) force coefficients during pitching motions of NACA0021 airfoil with a maximum amplitude of 13.8° (analog to $\lambda = 4.19$).

4.2. Turbulence model comparison

A simulation with a RANS k-ϵ standard turbulence model was carried out to compare the obtained results against another one using a LES Smagorinsky turbulence model. Figure 10

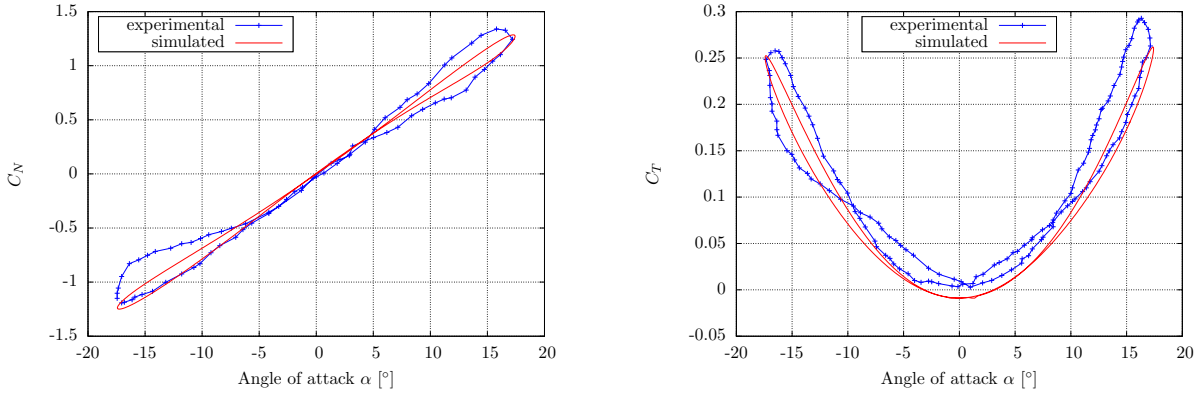

Figure 8. Normal (left) and tangential (right) force coefficients during pitching motions of NACA0021 airfoil with a maximum amplitude of 17.4° (analog to $\lambda = 3.34$).

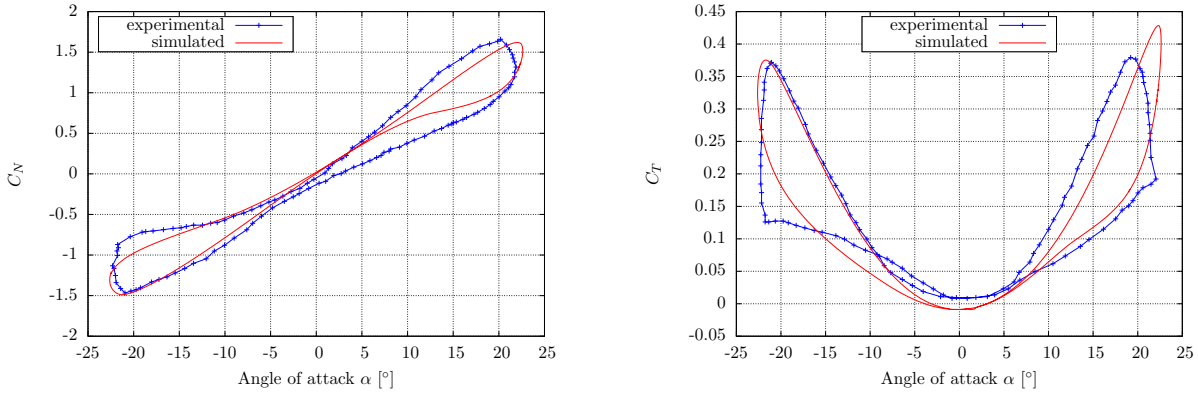

Figure 9. Normal (left) and tangential (right) force coefficients during pitching motions of NACA0021 airfoil with a maximum amplitude of 22.6° (analog to $\lambda = 2.60$).

shows that for the C_N values there is not considerable difference, but a small improvement has been achieved for the C_T values.

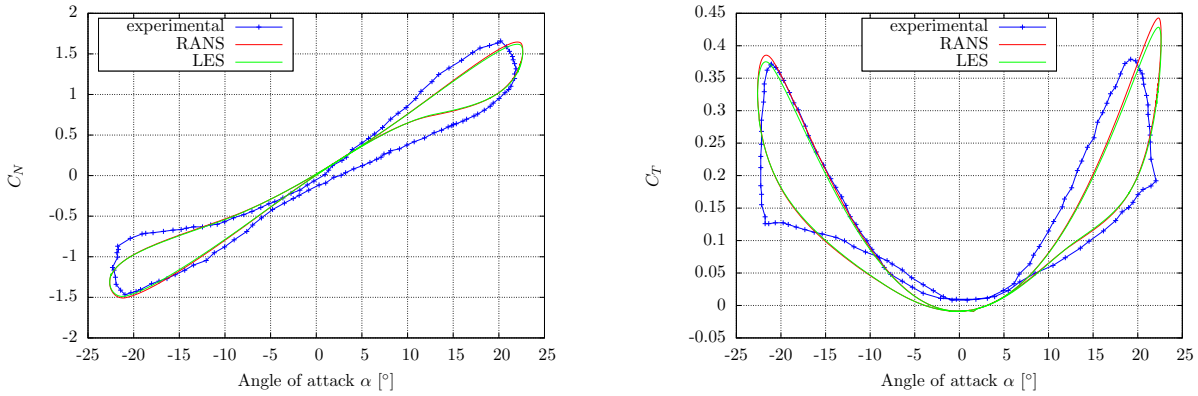

Figure 10. Normal (left) and tangential (right) force coefficients for different turbulence models, pitching motion with a maximum amplitude of 22.6°

4.3. Unsteady effects correction

According to [13], where the dynamic stall model is combined with a vortex model, it is beneficial to omit the attached flow correction equation 5 and instead use $\alpha_E = \alpha_n$. Hence, it is of interest to investigate if this correction should be included or not when the ALM is used instead of the vortex model. Figure 11 depicts that simulated results with the attached flow corrections have small improvements in the accuracy and are closer to experimental data. Results without corrections also have good agreement. Both C_N and C_T peak values are not overestimated. This has also been tested for larger angles of attack and the differences between using equation 5 or not are less significant here as the separated flow modeling dominates the force calculation.

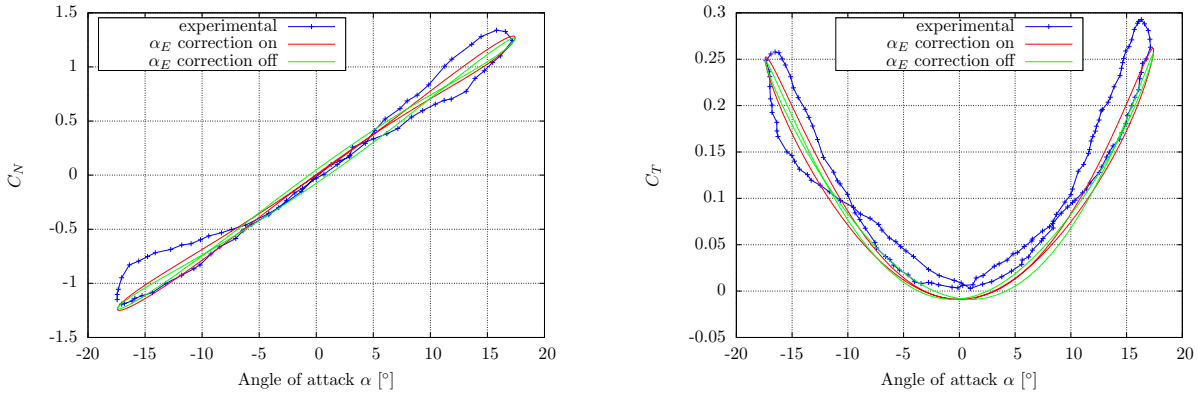

Figure 11. Normal (left) and tangential (right) force coefficients with and without unsteady effects correction, pitching motion with a maximum amplitude of 17.4°

5. Conclusions

It has been demonstrated that the presented coupled model ALM with DSM, shows good agreement with experimental data, considering the complexity of the flows studied. Moreover, the model has been tested for a wide range of pitching amplitudes, therefore, with different stall conditions (none, shallow, and deep stall), results agreed well compared with experiments. The model is stable and accurate for the tested pitching blade motions, which makes it suitable for application in VAWT simulations.

Acknowledgment

Financial support from STandUP for Energy and Uppsala University, are gratefully acknowledged.

References

[1] S.A. Huyer, D. Simms, and M.C. Robinson. Unsteady aerodynamics associated with a horizontal-axis wind turbine. *AIAA journal*, 34(7):1410–1419, 1996.

[2] J.N. Sørensen and W.Z. Shen. Computation of wind turbine wakes using combined navier-stokes/actuator-line methodology. In *Proceedings of European Wind Energy Conference Ewec'99, Nice*, 1999.

[3] P. Bachant and M. Wosnik. Simulating wind and marine hydrokinetic turbines with actuator lines in rans and les. *Bulletin of the American Physical Society*, 60, 2015.

[4] P. Bachant, A. Goude, and M. Wosnik. Actuator line modeling of vertical-axis turbines. *arXiv preprint arXiv:1605.01449 Submitted to Wind Energy*, 2016.

[5] Peter Bachant, Anders Goude, and Martin Wosnik. turbinesFoam: v0.0.7. Zenodo. http://dx.doi.org/10.5281/zenodo.49422, 2016.

[6] R. E. Sheldahl and P. C. Klimas. Aerodynamic characteristics of seven symmetrical airfoil sections through 180-degree angle of attack for use in aerodynamic analysis of vertical axis wind turbines. Technical report, Sandia National Labs., Albuquerque, NM (USA), 1981.

[7] J.G. Leishman and T.S. Beddoes. A generalised model for airfoil unsteady aerodynamic behaviour and dynamic stall using the indicial method. In *Proceedings of the 42nd Annual forum of the American Helicopter Society*, pages 243–265. Washington DC, 1986.

[8] W. Sheng, R.A. Galbraith, and F.N. Coton. A modified dynamic stall model for low mach numbers. *Journal of Solar Energy Engineering*, 130(3):031013, 2008.

[9] E. Dyachuk. Aerodynamics of vertical axis wind turbines: Development of simulation tools and experiments. 2015.

[10] J.G. Leishman and T.S. Beddoes. A semi-empirical model for dynamic stall. *Journal of the American Helicopter society*, 34(3):3–17, 1989.

[11] E. Dyachuk, A. Goude, and H. Bernhoff. Dynamic stall modeling for the conditions of vertical axis wind turbines. *AIAA journal*, 52(1):72–81, 2013.

[12] R.K. Angell, P. Musgrove, R.A.M.D. Galbraith, University of Glasgow. Department of Aeronautics, and Fluid Mechanics. *The Collected Data for Tests on a NACA 0021 Aerofoil*. G. U. Aero report. University of Glasgow, Department of Aeronautics & Fluid Mechanics, 1988.

[13] E. Dyachuk, A. Goude, and H. Bernhoff. Simulating pitching blade with free vortex model coupled with dynamic stall model for conditions of straight bladed vertical axis turbines. *Journal of Solar Energy Engineering*, 137(4):041008, 2015.